 doi:10.1111/j.1471-4159.2004.02888.x

Synaptopodin, a molecule involved in the formation of the dendritic spine apparatus, is a dual actin/α-actinin binding protein

Joachim Kremerskothen,* Christian Plaas,* Stefan Kindler,† Michael Frotscher‡ and Angelika Barnekow*

**Department for Experimental Tumorbiology, University of Muenster, Muenster, Germany*

†*Institute for Cell Biochemistry and Clinical Neurobiology and Institute for Human Genetics, University Hospital Hamburg-Eppendorf, Hamburg, Germany*

‡*Institute of Anatomy and Cell Biology, University of Freiburg, Germany*

Abstract

Synaptopodin (SYNPO) is a cytoskeletal protein that is preferentially located in mature dendritic spines, where it accumulates in the spine neck and closely associates with the spine apparatus. Formation of the spine apparatus critically depends on SYNPO. To further determine its molecular action, we screened for cellular binding partners. Using the yeast two-hybrid system and biochemical assays, SYNPO was found to associate with both F-actin and α-actinin. Ectopic expression of SYNPO in neuronal and non-neuronal cells induced actin aggregates, thus confirming a cytoplasmic interaction with the actin cytoskeleton. Whereas F-actin association is mediated by a central SYNPO motif, binding to α-actinin requires the C-terminal domain. Notably, the α-actinin binding domain is also essential for dendritic targeting and postsynaptic accumulation of SYNPO in primary neurons. Taken together, our data suggest that dendritic spine accumulation of SYNPO critically depends on its interaction with postsynaptic α-actinin and that SYNPO may regulate spine morphology, motility and function via its distinct modes of association with the actin cytoskeleton.

Keywords: postsynaptic cytoskeleton, spine apparatus, synaptic plasticity.

J. Neurochem. (2005) 10.1111/j.1471-4159.2004.02888.x

Dendritic spines behave as individual postsynaptic compartments regulating synaptic plasticity (reviewed in Hering and Sheng 2001; Yuste and Bonhoeffer 2001; Sheng and Kim 2002; Lamprecht and LeDoux 2004). The spine shape undergoes rapid changes in response to synaptic activity as a result of the dynamic remodelling of the postsynaptic cytoskeleton (Engert and Bonhoeffer 1999; Toni *et al*. 1999; Matus 2000; Harris *et al*. 2003). Mechanisms that regulate the activity-dependent restructuring of the postsynaptic cytoskeleton are poorly understood. The spine apparatus (SA) represents a specialization of the smooth endoplasmic reticulum (SER) and is composed of electron dense plates as well as membranous cisternae (Gray 1959; Fifkova *et al*. 1983; Spacek 1985; Deller *et al*. 2000a,b, 2003). This organelle is present in many telencephalic spines that have a perforated synapse, i.e. the mushroom spines (Spacek 1985; Spacek and Harris 1997; Deller *et al*. 2000a,b, 2003). Synaptopodin (SYNPO) is an F-actin-associated protein located preferentially at the SA in spines of the telencephalon (Mundel *et al*. 1997; Deller *et al*. 2000a,b). Recent studies on SYNPO-deficient mice show that the protein is necessary for SA formation (Deller *et al*. 2003). Synaptic activity leads to elevated SYNPO protein synthesis in the hippocampus and distinct cortical regions, suggesting that SYNPO is involved in synaptic plasticity (Yamazaki *et al*. 2001; Fukazawa *et al*. 2003). Consistently, SYNPO knockout mice exhibit impaired long-term potentiation (LTP) and learning (Deller *et al*. 2003). To

Received June 18, 2004; revised manuscript received September 9, 2004; accepted September 25, 2004.

Address correspondence and reprint requests to Joachim Kremerskothen, Department for Experimental Tumorbiology, University of Muenster, Badestrasse 9, D-48149 Muenster, Germany.

E-mail: kremers@uni-muenster.de

Abbreviations used: CH, calponin homology; EGFP, enhanced-green fluorescence protein; FCS, fetal calf serum; GST, glutathion-S-transferase; LTP, long-term potentiation; PB, phosphate buffer; PBS, phosphate-buffered saline; SA, spine apparatus; SDS–PAGE, sodium dodecyl sulfate – polyacrylamide gel electrophoresis; SER, smooth endoplasmic reticulum; SYNPO, synaptopodin; TBS, Tris-buffered saline.

further elucidate the cellular action of SYNPO, we analyzed its interaction with the postsynaptic cytoskeleton. Our data demonstrate that SYNPO not only binds directly to F-actin but also interacts with the actin-bundling protein α-actinin that is enriched at the SA. The proline-rich carboxyterminus of SYNPO mediates both α-actinin binding and postsynaptic targeting. Overexpression of SYNPO leads to the formation of actin aggregates. This scaffolding activity depends on the association of SYNPO with both F-actin and α-actinin. In summary, our data indicate that SYNPO is a dual actin/α-actinin binding protein with a potential structural function in SA formation and spine architecture.

Materials and methods

Animals

Three adult mice (129/C57BL6; 25–30 g) housed under standard laboratory conditions were used for immunocytochemistry (see below).

Plasmids

Human SYNPO (KIAA1029, GenBank Acc. No. BAA82981), and α-actinin 1/2 cDNA fragments were cloned into yeast two-hybrid vectors pAS2-1, pACTII (Clontech, Heidelberg, Germany), eukaryotic expression vectors pSV42-HA (Weide *et al*. 2001), pEGFP (Clontech) and the bacterial expression vector pGEX-KG. Details of constructs and cloning procedures are given in Table 1.

Antibodies

Monoclonal antibodies directed against SYNPO (G1D4), α-actinin 2 (EA-53) and PSD-95 (7B3–1B8) were purchased from Progen (Heidelberg, Germany), Upstate Biotechnology (Lake Placid, NY, USA) and Sigma (Deisenhofen, Germany), respectively. Anti-enhanced-green fluorescence protein (EGFP) antibodies were from BD Biosciences (Heidelberg, Germany). Polyclonal antibodies against α-actinin 2 were a kind gift from M. Sheng (Massachusetts Institute of Technology, Boston, MA, USA). Horseradish-peroxidase and fluorochrome conjugated secondary antibodies as well as phalloidin-fluorochrome conjugates were purchased from Amersham-Biosciences (Freiburg, Germany) and Molecular Probes (Karlsruhe, Germany), respectively.

In vitro synthesis of radioactively labelled SYNPO

^{35}S-labelled SYNPO was synthesized from pSV42-HA-SYNPO using the TNT coupled reticulocyte lysate system (Promega, Heidelberg, Germany) according to the manufacturer's instructions.

Actin co-sedimentation assay

Actin co-sedimentation assays were performed as described previously (Kaplan *et al*. 2000). ^{35}S-labelled SYNPO was incubated with purified F-actin (a generous gift from D. Koehler, University of Muenster) in sedimentation buffer (10 mM HEPES pH 7.4, 30 mM KCl, 2 mM $MgCl_2$, 1 mM EGTA, 1 mM β-mercaptoethanol) and was centrifuged thereafter for 1 h at 100 000 *g*. The supernatants and the pellets were resolved in 1 × sodium dodecyl sulfate (SDS) sample buffer (Laemmli 1970) and proteins were separated by SDS–polyacrylamid gel electrophoresis (PAGE). Distribution of actin was determined by Coomassie Blue staining whereas ^{35}S-SYNPO was detected by fluorography.

Cell culture, transfections and immunocytochemistry

Culturing, transfection and immunocytochemistry of monkey CV1 kidney cells and primary rat hippocampal neurons were described previously (Blichenberg *et al*. 1999; Kremerskothen *et al*. 2003). In brief, CV1 cells were grown on coverslips in Dulbecco's modified Eagle medium (DMEM) supplemented with 10% fetal calf serum (FCS) at 37°C in 5% CO_2/95% O_2. For transient expression, CV1 cells were transfected with plasmids using PolyFect (Qiagen, Hilden, Germany) according to the manufacturer's instructions. One to two days after the transfection the medium was aspirated, culture dishes were washed three times with phosphate-buffered saline (PBS) and cells were used for immunocytochemistry.

Rat hippocampal neurons were prepared at embryonic day 19 and plated at a density of about 500 cells/mm^2. Cultures were grown on coverslips in neurobasal medium (Invitrogen, Heidelberg, Germany) supplemented with B27 (Invitrogen) and 0.5 mM glutamine. Glutamate (12.5 μM) was included for the first 4 days in culture. Seven days after plating cells were transfected using a modified calcium phosphate precipitation protocol (Blichenberg *et al*. 1999). One to three days after transfection, neurons were analyzed by immunocytochemistry.

For immunocytochemistry, cells were fixed in 4% paraformaldehyd in PBS at room temperature (20°C) for 15 min, and blocked with 10% (v/v) FCS in PBS for 30 min. Immunofluorescence staining was done by incubating the coverslips for 1 h at room temperature with primary antibodies diluted in 10% (v/v) FCS in PBS. After three washes in PBS, coverslips were incubated 30 min at room temperature with fluorochrome-conjugated secondary antibodies diluted in 10% (v/v) FCS in PBS. After three washes in PBS, cells were mounted and photographed using a Leica TCS NT confocal microscope.

Perfusion of mice and preparation of tissue sections

Mice were perfused through the heart under deep Narcodorm-n anaesthesia (0.3 mL/100 g), first with 0.9% NaCl and then with 100 mL fixative containing 0.1% glutaraldehyde (Polysciences Inc., Warrington, PA, USA), 4% paraformaldehyde (Merck, Darmstadt, Germany) and 0.2% picric acid in 0.1 M phosphate buffer (PB; pH 7.4). Experiments were performed in agreement with the German law on the use of laboratory animals. After fixation, brains were removed from the skull and post-fixed in the same fixative for 2 h. Frontal sections of the hippocampus were cut on a vibratome at 50 μm. After extensive washes in PB, the sections were immersed in a solution of 10% glycerol and 25% sucrose in PB and freeze-thawed in liquid nitrogen-cooled isopentane for 5–6 s. After repeated washing in PB, the sections were transferred to 0.05 M Tris-buffered saline (TBS).

Pre-embedding immunocytochemistry

Sections were first incubated in 10% normal goat serum for 1 h, and then in the primary antiserum (mouse anti-α-actinin 2, EA-53; 1 : 250) for 2 days at 4°C. All washing steps and the dilution of the antisera were performed in 50 mM TBS (pH 7.4). The sections were

Table 1 Plasmids used in the experiments

Construct	Parental vector	Insert	Cloning sites	Use
pSV42–HA–SYNPO	pSV42–HA (Weide *et al.* 2001)	Human SYNPO cDNA, encodes aa 1–903	*Nde*I/*Xho*I	*In vitro* transcription/ translation
pEGFP–SYNPO$_{1-903}$	Modified pEGFP–C2 (Clontech)	Human SYNPO cDNA, encodes aa 1–903	*Nde*I/*Xho*I	Transfection
pEGFP–SYNPO$_{1-483}$	Modified pEGFP–C2 (Clontech)	Human SYNPO cDNA, encodes aa 1–483	*Nde*I/*Sac*I	Transfection
pEGFP–SYNPO$_{1-245}$	modified pEGFP–C2 (Clontech)	Human SYNPO cDNA, encodes aa 1–245	*Nde*I/*Bam*HI	Transfection
pEGFP–SYNPO$_{245-483}$	pEGFP–C3 (Clontech)	Human SYNPO cDNA, encodes aa 245–483	*Bgl*II/*Sac*I	Transfection
pEGFP–SYNPO$_{391-483}$	pEGFP–C3 (Clontech)	Human SYNPO cDNA, encodes aa 391–483	*Bgl*II/*Sac*I	Transfection
pEGFP–SYNPO$_{483-903}$	pEGFP–C3 (Clontech)	Human SYNPO cDNA, encodes aa 483–903	*Sac*I/*Sal*I	Transfection
pEGFP–SYNPO$_{483-752}$	pEGFP–C3 (Clontech)	Human SYNPO cDNA, encodes aa 483–752	*Sac*I/*Pst*I	Transfection
pEGFP–SYNPO$_{1-752}$	Modified pEGFP–C2 (Clontech)	Human SYNPO cDNA, encodes aa 1–752	*Nde*I/*Pst*I	Transfection
pEGFP–SYNPO$_{752-903}$	pEGFP–C3 (Clontech)	Human SYNPO cDNA, encodes aa 752–903	*Pst*I	Transfection
pAS–SYNPO$_{1-903}$	pAS2–1 (Clontech)	Human SYNPO cDNA, encodes aa 1–903	*Nde*I/*Sal*I	Yeast two-hybrid system
pAS–SYNPO$_{1-245}$	pAS2–1 (Clontech)	Human SYNPO cDNA, encodes aa 1–245	*Nde*I/*Bam*HI	Yeast two-hybrid system
pAS–SYNPO$_{245-483}$	pAS2–1 (Clontech)	Human SYNPO cDNA, encodes aa 245–483	*Bam*HI/*Sal*I	Yeast two-hybrid system
pAS–SYNPO$_{483-903}$	pAS2–1 (Clontech)	Human SYNPO cDNA, encodes aa 483–903	*Nde*I/*Sal*I	Yeast two-hybrid system
pAS–SYNPO$_{483-752}$	pAS2–1 (Clontech)	Human SYNPO cDNA, encodes aa 483–752	*Nde*I/*Pst*I	Yeast Two-Hybrid system
pAS–SYNPO$_{635-903}$	pAS2–1 (Clontech)	Human SYNPO cDNA, encodes aa 635–903	*Pst*I	Yeast two-hybrid system
pACT–actinin 1	pACTII (Clontech)	Human α-actinin 1 cDNA, encodes aa 1–892	*Eco*RI/*Xho*I	Yeast two-hybrid system
pACT–actinin 2	pACTII (Clontech)	Human α-actinin 2 cDNA, encodes aa 1–894	*Eco*RI/*Xho*I	Yeast two-hybrid system
pACT–Spec1–4	pACTII (Clontech)	Human α-actinin 1 cDNA, encodes aa 245–726	*Eco*RI/*Xho*I	Yeast two-hybrid system
pACT–Spec1–3	pACTII (Clontech)	Human α-actinin 1 cDNA, encodes aa 245–599	*Eco*RI/*Xho*I	Yeast two-hybrid system
pACT–Spec-C	pACTII (Clontech)	Human α-actinin 1 cDNA, encodes aa 570–750	*Eco*RI/*Xho*I	Yeast two-hybrid system
pACT–EF hands	pACTII (Clontech)	Human α-actinin 1 cDNA, encodes aa 750–892	*Eco*RI/*Xho*I	Yeast two-hybrid system
pGEX–KG–Spec1–4	pGEX–KG	Human α-actinin 1 cDNA, encodes aa 245–726	*Eco*RI/*Xho*I	Bacterial expression, GST pull down

aa, amino acids.

then incubated in Nanogold^{R}-anti-mouse (1.4 nm, 1 : 100; Nanoprobes, NY, USA) at 4°C overnight. Following incubation in 1% glutaraldehyde in 0.025 M TBS and washing in distilled water, the staining was intensified with HQ Silver^{TM} Enhancement Kit (Nanoprobes) for 5 min. After osmium tetroxide treatment (1% OsO_4 in 0.1 M PB for 30 min), the sections were dehydrated in an ascending series of ethanol (1% uranyl acetate contained in 70% ethanol) and propylene oxide, and flat-embedded in Durcupan (ACM, Fluka, Seelze, Germany). Ultrathin sections were examined in a CM 100 Philips electron microscope.

Preparation of mouse brain extract and co-immunoprecipitation assays

Preparation of brain extracts from adult mice and co-immunoprecipitation experiments were performed as described earlier by Patrie *et al*. (2002). Briefly, mouse brains were placed in a Dounce homogenizer along with high-salt Triton lysis buffer (50 mM Hepes (pH 7.5), 500 mM NaCl, 1.5 mM $MgCl_2$, 1 mM ethyleneglycol-O,O′-bis-[2-aminoethyl]-*N*,*N*,*N*′,*N*′,-tetra-acetic acid (EGTA), 10% glycerol, and 1% Triton X-100) plus protease inhibitors (Complete protease inhibitor mixture tablets, Roche, Mannheim, Germany) and homogenized with 25–30 strokes. The lysates were centrifuged at 20 000 *g* for 60 min at 4°C, and the supernatants were transferred to fresh tubes and stored at −70°C until used. Protein concentrations of the samples were determined by the BCA assay according to the manufacturer's instructions (Perbio, Bonn, Germany).

For immunoprecipitations, aliquots of the lysates (corresponding to 100 μg protein) were brought up to a total volume of 500 μL with low-salt lysis buffer containing 100 mM NaCl and rocked overnight at 4°C with anti-α-actinin 2 (EA-53) or control IgG antibodies, respectively. The following day, protein A-Sepharose beads (15 μL) were added to the samples and rocked for an additional 1 h at 4°C. The beads were then washed four times in low-salt lysis buffer. After the supernatants were removed, 30 μL of 1 × SDS sample buffer were added to the beads. The samples were boiled for 5 min and proteins eluted off the beads, together with aliquots (2%) of the starting lysate, were subjected to SDS–PAGE, transferred to a polyvinylidene difluoride (PVDF) membrane, and incubated subsequently with the appropriate primary and horseradish peroxidase-conjugated secondary antibodies. Blots were then developed with chemiluminescence reagents (Perbio) and exposed to X-ray films.

Recombinant proteins and glutathion-S-transferase (GST) pull downs

A pGEX-KG construct containing the cDNA encoding Spec1-4 from α-actinin 1 (see Table 1) was used for the isopropyl-β-D-thiogalactopyranoside (IPTG)-induced expression of GST fusion proteins in *Escherichia coli* BL21. Recombinant proteins were isolated from bacterial lysates with glutathione-sepharose beads (Amersham Biosciences, Freiburg, Germany) according to the manufacturer's instructions. Brain lysates (corresponding to 100 μg protein) were combined with approximately 5 μg of GST fusion proteins or GST immobilized on glutathione-sepharose beads and incubated overnight at 4°C. Beads were washed extensively with low-salt lysis buffer (see above), bound proteins were eluted by boiling in 1 × SDS sample buffer, subjected together with 5% of the input to SDS–PAGE and analyzed by western blotting.

Yeast two-hybrid methods

In order to test the specificity of the interaction between fragments of human SYNPO and α-actinin, Y190 yeast cells were co-transformed using various bait and prey constructs (see Table 1) and incubated on selection plates at 30°C for 7 days according to the manufacturer's instructions (Matchmarker II System, BD Biosciences Clontech, Heidelberg, Germany). A protein/protein interaction was confirmed by growth on selective media and β-galactosidase filter lift assays using X-gal as substrate (Weide *et al*. 2001). All bait and prey constructs were tested for autocatalytic activity.

Results

SYNPO is an autonomous actin-binding protein

The formerly published mouse SYNPO cDNA sequence encodes a protein of 692 amino acids with a predicted molecular weight of 74 kDa (Mundel *et al*. 1997). However, anti-SYNPO antibodies detect proteins of 100 and 110 kDa in mouse brain and kidney extracts, respectively (Mundel *et al*. 1997), suggesting that the published sequence may be incomplete. Human cDNA clone KIAA1029 (GenBank Accession No. AB028952) contains an open reading frame that encodes a 903-amino acid protein, with a calculated molecular mass of 96.4 kDa. The *in vitro* synthesized human protein (KIAA1029) co-migrates with endogenous mouse brain SYNPO (Fig. 1a), indicating that it represents full-length SYNPO. Whereas the amino-terminal part of the human protein is highly homologous to mouse SYNPO, it contains an elongated carboxyterminus that is also encoded by a recently described mouse cDNA clone (GenBank Accession No. XM_129030, Fig. 1d) showing that the longer SYNPO isoform is also present in the mouse.

Based on the findings that SYNPO is distributed along actin fibres and that this localization is sensitive to actin-depolymeriation reagents, it was postulated that SYNPO binds to F-actin (Mundel *et al*. 1997). Here, we show that, in a co-sedimentation assay (Kaplan *et al*. 2000), ^{35}S-labelled SYNPO is quantitatively sedimented in the presence (Fig. 1a, lanes 3 and 4) but not in the absence (lanes 1 and 2) of F-actin, thus demonstrating direct binding of SYNPO to F-actin.

To determine its actin-binding site(s), several SYNPO fragments were transiently expressed as enhanced-green fluorescence protein (EGFP)-fusion proteins in monkey CV1 cells and their association with F-actin was analyzed by indirect immunocytochemistry. Similar to full-length SYNPO, EGFP–$SYNPO_{483–903}$ and EGFP–$SYNPO_{752–903}$ exhibited a punctuated distribution along actin stress fibres (Fig. 1b, i, vi and ix). In contrast, EGFP–$SYNPO_{1–483}$, EGFP–$SYNPO_{1–752}$, EGFP–$SYNPO_{245–483}$, and EGFP–$SYNPO_{391–483}$ displayed a more homogenous decoration of actin filaments (Fig. 1b, ii, iv, v and viii), whereas EGFP–$SYNPO_{1–245}$ and EGFP–$SYNPO_{483–752}$ did not associate with the actin cytoskeleton but were diffusely distributed in the cytoplasm of transfected cells (Fig. 1b, iii and vii). Thus, SYNPO appears to contain at least two domains, which both independently mediate an interaction with microfilaments. Whereas the region spanning amino acid residues nos 391–485 leads to a homogenous association with actin filaments, amino acids nos 792–903 are necessary for a punctuated pattern of SYNPO along microfilaments (for a summary see Fig. 1e). It is worth noting, that the amino-terminal actin-binding motif is similar to a functionally related domain in

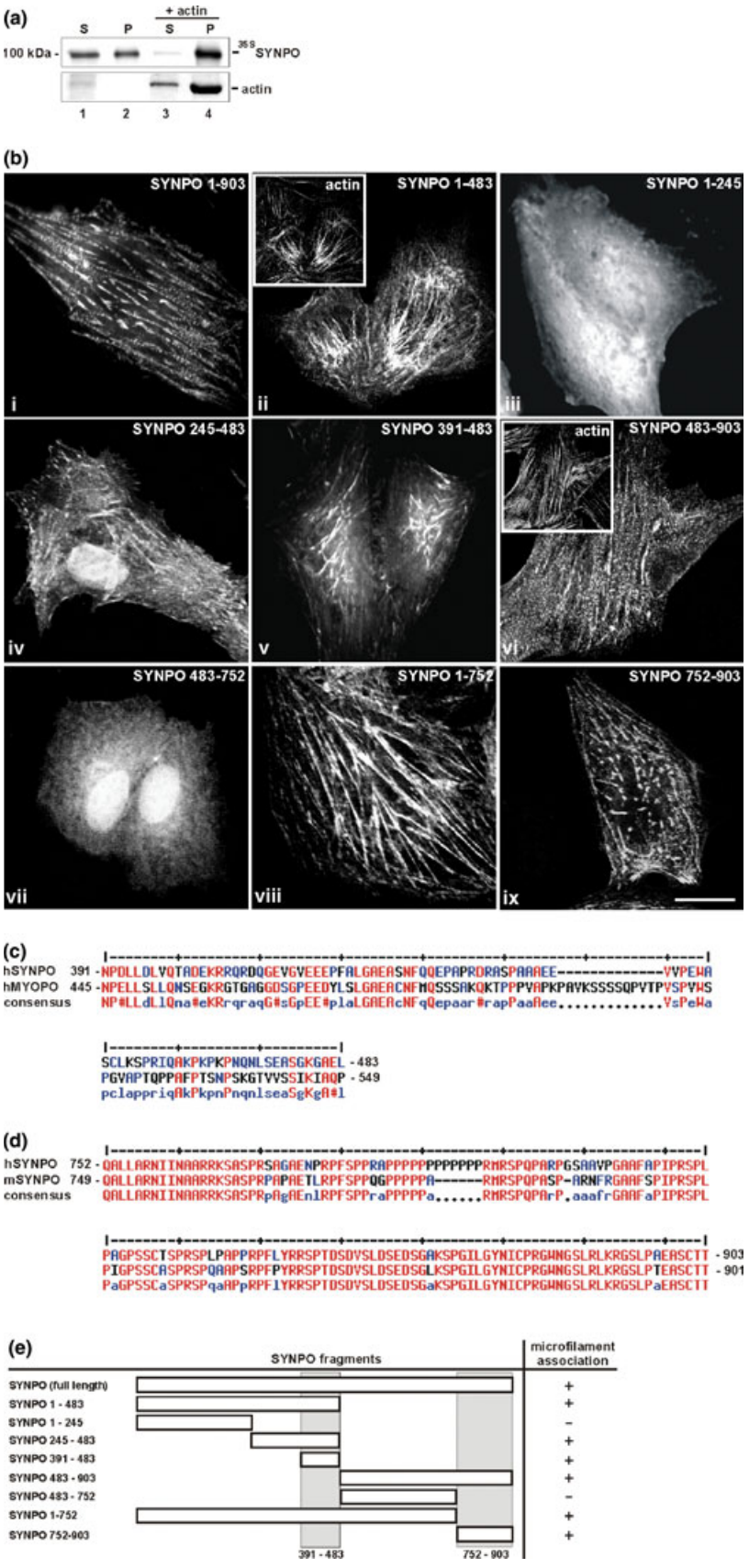

Fig. 1 SYNPO associates with actin through two binding sites. (a) For co-sedimentation assays, ^{35}S-labelled SYNPO (100 kDa) was incubated in sedimentation buffer in the presence (lanes 3 and 4) or absence of F-actin (lanes 1 and 2). After ultracentrifugation, the supernatants (S) as well as the pellets (P) were diluted in sample buffer and were subjected to SDS–PAGE. ^{35}S-SYNPO was detected by fluorography of the dried gel, whereas actin was stained with Coomassie Blue. In the presence of F-actin, ^{35}S-SYNPO was mainly transferred to the pellet fraction, indicating a direct interaction. (b) CV1 cells were transiently transfected with constructs encoding various SYNPO fragments fused to EGFP. Confocal microscopy of the fixed cells revealed that SYNPO contains two motifs for the association with actin. The first internal motif includes amino acids 391–483 (Fig. 1b, i, ii, iv, v and viii), whereas the second motif represents the carboxyterminus of SYNPO spanning from amino acids 752–903 (Fig. 1b, vi and ix). EGFP fusion proteins lacking both motifs display a diffuse distribution in the cytoplasm and in the nuclei of transfected cells [Fig. 1b, iii (EGFP–SYNPO$_{1-245}$) and Fig. 1b, vii (EGFP–SYNPO$_{483-752}$)]. Expression of SYNPO fragments does not alter the structure of the actin cytoskeleton (exemplarily shown by Phalloidin staining of cells transfected with constructs encoding EGFP–SYNPO$_{1-483}$ or EGFP–SYNPO$_{483-903}$, insets in Fig. 1b, ii and vi). Scale bar represents 30 μm. (c) Sequence alignment of the actin binding sites from SYNPO and myopodin demonstrated a moderate level of similarity. High consensus amino acids are marked by red letters, low consensus amino acids are indicated by black and blue letters. Numbers give the position of amino acids in the SYNPO and in the myopodin sequence, respectively. (d) Alignment of the SYNPO carboxyterminal amino acid sequence from mouse and human. (e) Summary of the transfection experiments using different SYNPO fragments fused to EGFP. SYNPO contains two microfilament association sites that are located between amino acids 391–483 and amino acids 752–903, respectively.

myopodin, the second member of the SYNPO gene family (Weins *et al*. 2001; Fig. 1c).

SYNPO binds to α-actinin

The punctuated distribution of SYNPO along actin fibres very much resembles the pattern of microfilament-associated α-actinin (Mundel *et al*. 1997). Furthermore, a co-localization of SYNPO and α-actinin in podocytes has been previously demonstrated (Ichimura *et al*. 2003; Kos *et al*. 2003; Goode *et al*. 2004). We therefore analyzed a putative direct association of SYNPO with α-actinin using the yeast two-hybrid system. Co-transformation assays revealed a strong interaction between SYNPO and the postsynaptic α-actinin isoforms 1 and 2 as shown by the activation of reporter genes (Fig. 2). α-Actinin has a modular structure consisting of two calponin homology (CH) domains, a central rod domain containing four spectrin (Spec) repeats, and two C-terminal EF hand motifs (Blanchard *et al*. 1989; Kremerskothen *et al*. 2002). Deletion analysis demonstrated that spectrin repeats 1–4 are sufficient and spectrin domain 4 (Spec4) is necessary for SYNPO binding (Fig. 2).

The α-actinin binding site of SYNPO was mapped to the carboxyterminus of the protein between amino acids 752 and 903 (Fig. 2). Whereas SYNPO amino acids 483–903 were sufficient for an association with α-actinin, SYNPO amino acids 752–903 were necessary for the interaction. Only SYNPO constructs containing this sequence domain ($SYNPO_{483-903}$, $SYNPO_{635-903}$) but not those lacking this part of SYNPO ($SYNPO_{1-245}$, $SYNPO_{245-483}$, $SYNPO_{483-752}$) were able to interact with α-actinin in co-transformation experiments. Interestingly, subparts of the carboxyterminus ($SYNPO_{752-903}$) did not interact with α-actinin, indicating that amino acids 752–903 represent the minimal binding domain (data not shown).

The yeast data were further verified using *in vitro* GST pull-down assays with a mouse brain extract. GST fused to spectrin domains 1–4 of α-actinin 1 (GST Spec1–4), but not GST alone, selectively pulled down SYNPO (Fig. 3a, lanes 2

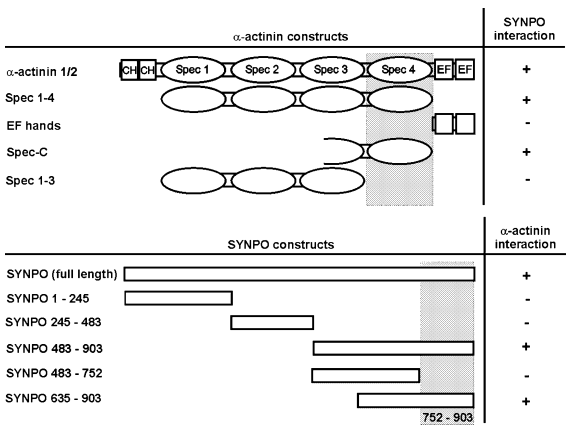

Fig. 2 SYNPO interacts with α-actinin in the yeast two-hybrid system. Yeast cells were co-transformed using various bait and prey constructs (see Table 1) and incubated on selection plates at 30°C for 7 days. A protein/protein interaction was confirmed by growth on selective media and β-galactosidase filter lift assays. The data revealed that SYNPO interacts strongly with α-actinin 1 and 2. Mapping of binding sites demonstrated that the fourth spectrin repeat (spec 4, amino acids 599–726) of α-actinin 1, but not the calponin-homology motif (CH, amino acids 1–245), spec 1–3 (amino acids 245–599) or the EF hands (EF, amino acids 750–892) mediate SYNPO interaction. The α-actinin 1-binding site on SYNPO was mapped to the carboxyterminus of the protein spanning from amino acids 752–903 that is included in SYNPO full length (1–903), SYNPO 483–903 and SYNPO 635–903. Fragments lacking this motif (SYNPO 1–245, SYNPO 245–483, SYNPO 483–752) did not interact with α-actinin.

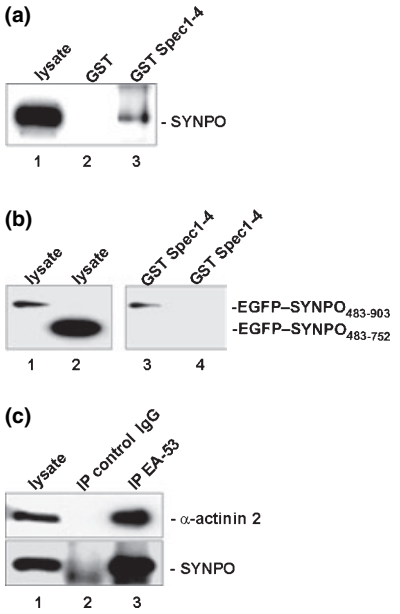

Fig. 3 *In vitro* interaction of SYNPO and α-actinin. (a) For pull-down experiments, bacterial expressed GST or GST-Spec1–4 fusion proteins (5 μg each) were incubated with mouse brain extract (100 μg). After the pull down, purified proteins were subjected to western blot analysis using anti-SYNPO antibodies. Whereas GST does not associate with SYNPO (lane 2), GST-Spec1–4 precipitates SYNPO from brain lysate (lane 3). In lane 1, 5% of the input lysate was loaded. (b) Interaction with the spectrin repeats from α-actinin requires the carboxyterminus of SYNPO (amino acids 752–903). Extracts from transiently transfected CV1 cells expressing EGFP–$SYNPO_{483-903}$ (lane 1) or EGFP–$SYNPO_{483-752}$ (lane 2) were incubated with GST-Spec1–4. After the pull down of the complexes, western blot analysis of 5% of each input (lanes 1 and 2) together with purified proteins (lanes 3 and 4) was performed with an anti-EGFP antibody (lanes 1–4). (c) Co-immunoprecipitation of SYNPO and α-actinin 2. Mouse brain extract (100 μg) was incubated with monoclonal α-actinin 2 antibodies (EA-53) or with normal mouse IgG. After precipitation of the complexes using sepharose-protein G beads, α-actinin 2 (top) and SYNPO (bottom) were detected by western blot analysis. In lane 1, 2% of the input lysate were loaded.

and 3). Moreover, GST Spec1–4 precipitated EGFP–SYNPO$_{483-903}$ (Fig. 3b, lanes 1 and 3) but not EGFP–SYNPO$_{483-752}$ (Fig. 3b, lanes 2 and 4) from extracts of transiently transfected CV1 cells, demonstrating again that the carboxyterminus of SYNPO spanning amino acids 752–903 is essential for the interaction with α-actinin.

Next, the *in vivo* interaction of SYNPO and α-actinin was determined by co-immunoprecipitation assays with mouse brain extracts. Immunoprecipitates obtained with antibodies against α-actinin 2 contained high amounts of SYNPO (Fig. 3c, lane 3), whereas this protein was not detected in precipitates acquired with control IgG antibodies (Fig. 3c, lane 2). Thus, SYNPO specifically associates *in vivo* with α-actinin 2.

The carboxyterminus containing the α-actinin-binding domain regulates the dendritic localization of SYNPO

Consistent with an *in vivo* interaction, SYNPO and α-actinin 2 co-localize along dendrites of cultured rat hippocampal neurons at putative synaptic sites (Fig. 4a, i–iii). In contrast to SYNPO, which displays a punctuated distribution at or near spines, α-actinin 2 was present in spines as well as in dendritic shafts in neurons at day 15 after plating. Three weeks after plating, SYNPO and α-actinin 2 co-localized in the heads of mushroom-like spines (arrowheads in Fig. 4a, iv–vi).

Electron microscopic immunogold labelling for α-actinin 2 further confirmed our co-localization studies. In thin sections, immunostaining for α-actinin 2 strongly labelled the spine apparatus of large dendritic spines in hippocampal region CA3 (Fig. 4b). Using a comparable immunogold protocol, we were recently able to demonstrate that SYNPO is similarly located to the spine apparatus (Deller *et al.* 2000a,b, 2003), confirming an interaction of the two proteins at the same cytoplasmic organelle.

To determine the postsynaptic targeting signal in SYNPO, we expressed various EGFP–SYNPO fragments in dissociated hippocampal neurons. Similar to full-length EGFP–

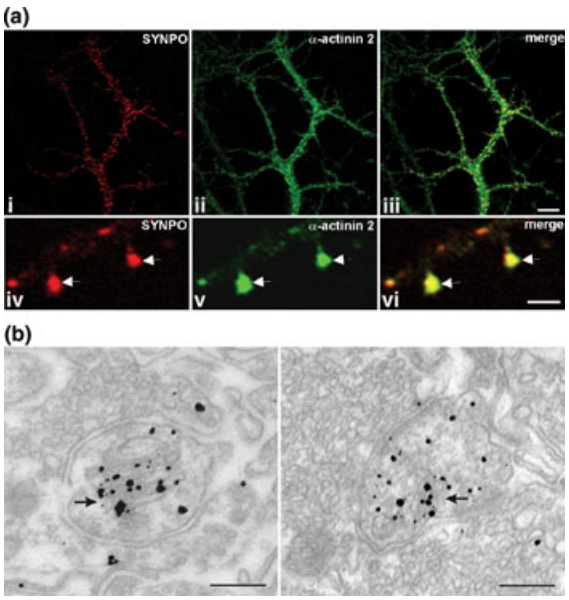

Fig. 4 Co-localization of SYNPO and α-actinin in dendrites of hippocampal neurons and ultrastructural localization of α-actinin at the SA of hippocampal spines. (a) Endogenous SYNPO (red) and α-actinin 2 (green) were stained by indirect immunocytochemistry in dissociated hippocampal neurons at day 15 (panels i–iii) or day 21 (panels iv–vi) after plating. Especially at day 21, both proteins co-localize at or near the head of mushroom-like spines (panels iv–vi, arrows). Scale bars represent 10 μm in (panels i–iii) and 3 μm in (panels iv–vi). (b) Two electron micrographs showing the ultrastructural localization of α-actinin 2 at the SA (arrows) of spines on CA3 pyramidal cell dendrites. Black dots represent silver-enhanced immunogold labelling for α-actinin 2. Scale bars represent 0.2 μm.

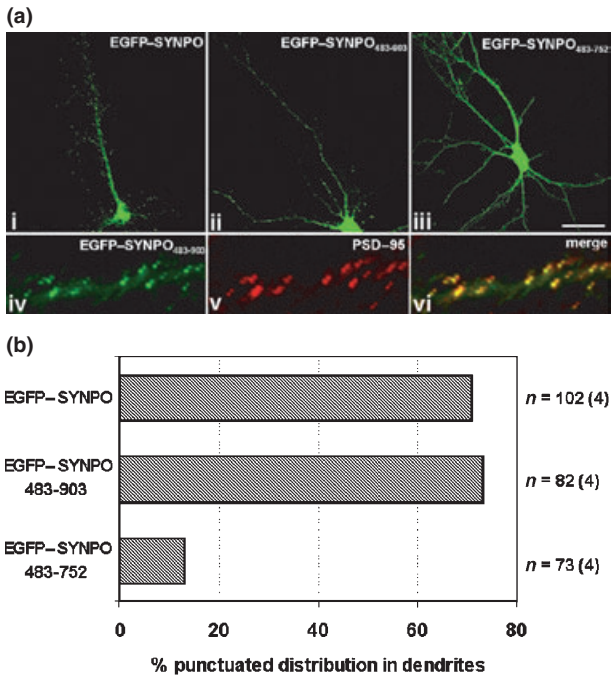

Fig. 5 The carboxyterminus of SYNPO containing the α-actinin-binding site mediates postsynaptic targeting. (a) Hippocampal neurons (7 days after plating) were transfected with constructs encoding SYNPO fragments fused to EGFP. Twenty-four hours after transfection, cells were fixed and analyzed by immunolabelling using confocal microscopy. Whereas full-length EGFP–SYNPO (a, i) and EGFP–SYNPO$_{483-903}$ (a, ii) were targeted to distinct dendritic sites, a mutant that lacks the carboxyterminus (EGFP–SYNPO$_{483-752}$) displays a diffuse distribution (a, iii). A co-staining of the postsynaptic marker PSD-95 (red) confirmed the postsynaptic localization of EGFP–SYNPO$_{483-903}$ (a, iv–vi, green). Scale bars represent 30 μm in panels i to iii and v μm in panels iv to vi, respectively. (b) Quantitative analysis of the localization of EGFP–SYNPO fusion proteins. The panel lists the relative amount of cells showing a punctuated (postsynaptic) localization of fusion proteins in dendrites of transfected hippocampal neurons, the total number of evaluated cells (*n*) and coverslips (in parentheses) per construct.

SYNPO, EGFP–SYNPO$_{483-903}$ was targeted to distinct sites on dendrites from transfected neurons (Fig. 5a, i and ii). Double immunofluorescence labelling with antibodies directed against the postsynaptic marker protein PSD-95 revealed co-localization and indicated a selective recruitment of EGFP–SYNPO$_{483-903}$ to postsynaptic sites (Fig. 5a, iv–vi). Deletion of the carboxyterminus of SYNPO containing the α-actinin-binding site disrupted synaptic targeting as shown by a homogenous cytoplasmic distribution of expressed EGFP–SYNPO$_{483-752}$ (Fig. 5a, iii). In addition, quantitative analysis of more than 250 transfected neurons clearly shows that amino acids 752–903 are necessary for a distinct dendritic localization of SYNPO (Fig. 5b).

SYNPO overexpression leads to formation of actin aggregates

Next, we analyzed the effect of SYNPO overexpression on the organization of the actin cytoskeleton. Enhanced synthesis of an EGFP–SYNPO fusion protein in CV1 cells led to significant changes of the actin cytoskeleton. Actin filaments were no longer distributed as parallel-orientated cables (inset in Fig. 6b) but displayed an aggregated and disorganized pattern (Fig. 6b, arrowheads). Frequently, aggregates that contained EGFP–SYNPO as well as actin were detected (Fig. 6c). This effect on actin arrangement was not seen in cells transfected with EGFP constructs that encoded SYNPO fragments lacking one or both actin association motifs (data not shown).

In hippocampal neurons, EGFP–SYNPO-containing aggregates were frequently found in the soma as well as in distal parts of dendrites (Fig. 6d–f). These aggregates did not only include actin but also α-actinin 2 as shown by indirect immunocytochemistry (Fig. 6g–l). Because the analyzed cells (10 days after plating) did not form mature spines, we were not able to analyze the effect of SYNPO overexpression on spine morphogenesis or spine cytoskeleton. Transfection of hippocampal neurons at later stages (day 14) or prolonged culture of transfected neurons (more than 3 days) gave no reliable results (data not shown).

Discussion

The spine apparatus (SA) is a postsynaptic organelle in the spines of mature neurons (Gray 1959; Spacek 1985; Spacek and Harris 1997; Deller 2000a,b). Whereas earlier data suggested that the SA acts as a calcium store in dendritic spines (Fifkova *et al*. 1983), recent studies pointed to a role in localized translation of dendritic mRNA (Golding and Segal 2003; McCarthy and Millner 2003). Several cytoskeleton-associated proteins have been identified as components

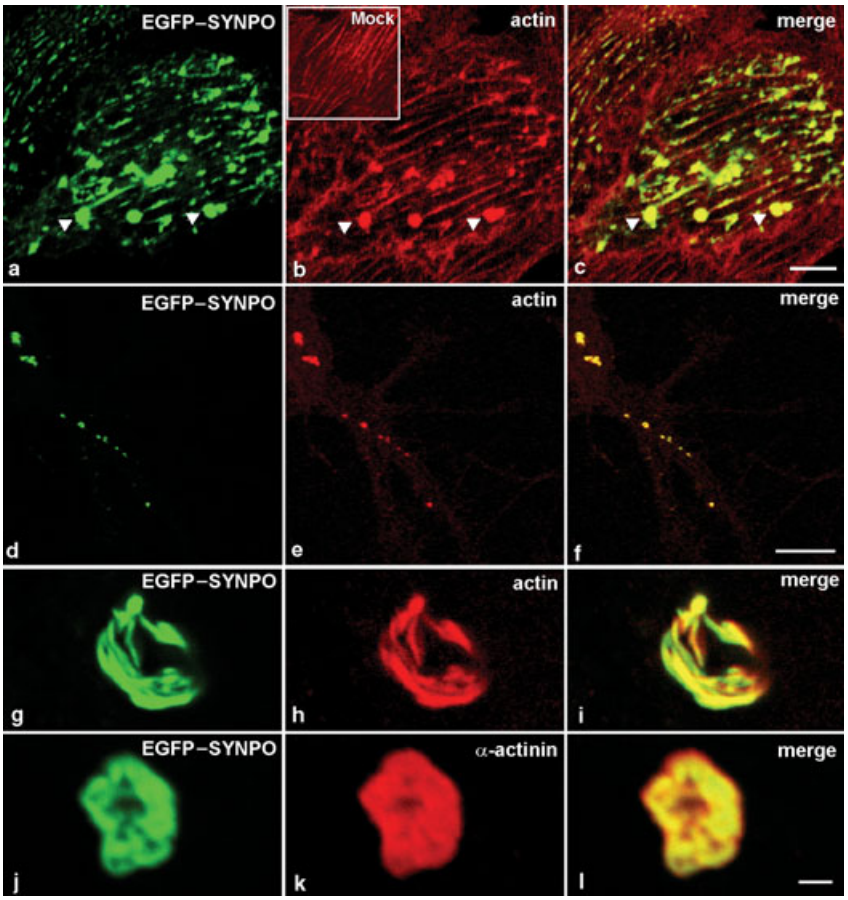

Fig. 6 Overexpression of SYNPO leads to actin aggregation. CV1 cells (a–c) or hippocampal neurons (d–l) were transfected with a construct encoding EGFP–SYNPO (full length). After 48 h (CV1) or 72 h (neurons), cells were fixed and the actin cytoskeleton was stained with a Phalloidin-Alexa 594 conjugate. Alternatively, α-actinin 2 was stained with EA-53 antibodies and a secondary antibody coupled to Alexa 594 (k, l, red). In CV1 cells, overexpressing of EGFP–SYNPO induces formation of actin aggregates (arrowheads) and reorganization of stress fibres (a–c). Inset in (b) shows the Phalloidin-Alexa 594-labelled actin stress fibres in a mock-transfected CV1 cell. In transfected hippocampal neurons, EGFP–SYNPO aggregates were frequently targeted to dendritic sites (d–f). High-resolution pictures of immunostained aggregates with a three-dimensional structure revealed that they contain SYNPO, actin and α-actinin (g–l). Bars represent 25 μm in (c) and (f) and 3 μm in (l), respectively.

of the SA, including F-actin, α-actinin and synaptopodin (SYNPO; Cohen *et al.* 1985; Wyszynski *et al*. 1998; Deller *et al*. 2000a,b). SYNPO-deficient mice completely lack the SA, indicating that SYNPO is essential for the formation of this organelle (Deller *et al*. 2003). The absence of enzymatic activity, the predicted rod-like structure of the protein and its proposed interaction with F-actin suggested a structural role of SYNPO. To prove this hypothesis, we analyzed the association of SYNPO with components of the postsynaptic cytoskeleton. Using *in vivo* as well as *in vitro* interaction assays, we were able to show that SYNPO not only binds to actin, but also to the actin-bundling molecule, α-actinin. Because SYNPO uses different binding sites for actin and α-actinin, a simultaneous binding of SYNPO to both molecules is likely. This implies that SYNPO may regulate and/or stabilize the interaction between actin and α-actinin in the SA, underlying the importance of these protein–protein interactions for SA formation.

Interestingly, myopodin, a protein highly similar to SYNPO, is predominately expressed in muscle cells, where it probably controls the architecture of the actin-based cytoskeleton and the assembly of the sarcomeric z-discs (Weins *et al*. 2001). Like SYNPO, myopodin interacts with actin and α-actinin and possesses actin-aggregation activity (Weins *et al*. 2001; D. Fürst and P. van der Ven, personal communication). These observations suggest that myopodin and SYNPO belong to a novel family of effector proteins that use similar mechanisms to interact with microfilaments.

We demonstrate that the carboxyterminal domain (amino acids 752–903) regulates the postsynaptic targeting of SYNPO (Fig. 5). This domain contains the interaction motif for α-actinin, which is highly enriched in dendritic spines and in the SA (Wyszynski *et al*. 1998; Walikonis *et al*. 2000; Fig. 4b). Although we cannot exclude that a second, yet unknown, protein binds to the SYNPO carboxyterminus, we postulate that postsynaptic localization of SYNPO depends on the interaction with α-actinin.

An interesting question is whether the association of actin and α-actinin with SYNPO affects the distribution of these cytoskeletal compounds in the spine. We postulate that SYNPO regulates actin/α-actinin localization specifically in the SA and not in other parts of the spine. Dissociated hippocampal neurons generate mature spines after about 2 weeks in culture. All of these spines contain high levels of actin and α-actinin, but only a subpopulation shows SYNPO expression (Mundel *et al*. 1997; Wyszynski *et al*. 1998; Deller *et al*. 2000a,b; Kremerskothen, data not shown). This indicates that SYNPO is not essential for a dendritic targeting of actin and α-actinin, but probably recruits theses cytoskeletal proteins from pools inside the spine for the formation of the SA. This model describing a SA-specific function of SYNPO is supported by an earlier ultrastructural analysis of telencaphalic neurons from SYNPO-deficient mice (Deller *et al*. 2003). Although the SA was completely missing in neurons from mutant mice, the number and size of dendritic spines were not altered, indicating the presence of a functional spine cytoskeleton (Deller *et al*. 2003). Unfortunately, an SA has never been observed in spines of dissociated neurons, even after a prolonged time in culture. Thus, it is currently not possible to study the significance of SYNPO for SA formation in cultured neurons.

Obviously, the formation of a complex containing SYNPO, actin and α-actinin is not sufficient to create an organelle like the SA consisting of cytoskeletal as well as membranous components. Therefore, other molecules that may associate directly or indirectly with SYNPO must be involved. Recent biochemical studies have shown that SYNPO binds to MAGI, a member of the family of MAGUK scaffolding proteins that are frequently enriched at postsynaptic sites (Dobrosotskaya *et al*. 1997; Hirao *et al*. 1998; Patrie *et al*. 2002). To further characterize the role of a SYNPO–MAGI complex in SA formation, it will be essential to analyze the putative co-localization of both proteins within the spine. Unfortunately, there are no anti-MAGI antibodies available that are suitable for an ultrastructural analysis.

The data reported here give first important insights into the function of SYNPO. Through an interaction with postsynaptic F-actin and α-actinin, SYNPO serves as an essential scaffolding component of the SA that probably recruits other molecules to this dendritic organelle. We are confident that our results about the interaction of SYNPO with components of the postsynaptic cytoskeleton will further help to elucidate the properties of the SA and its role in synaptic plasticity.

Acknowledgements

The authors thank S. Hirohashi, M. Sheng, and T. Nagase for plasmids or antibodies, M. Montenarh for CV1 cells, B. Schwanke for the preparation of hippocampal neurons and Aniko Schneider for her help with immunogold labelling.

References

Blanchard A., Ohanian V. and Critchley D. (1989) The structure and function of α-actinin. *J. Muscle Res. Cell Motil.* **10**, 280–289.

Blichenberg A., Schwanke B., Rehbein M., Garner C. C., Richter D. and Kindler S. (1999) Identification of a cis-acting dendritic targeting element in MAP2 mRNAs. *J. Neurosci.* **19**, 8818–8829.

Cohen R. S., Chung S. K. and Pfaff D. W. (1985) Immunocytochemical localization of actin in dendritic spines of the cerebral cortex using colloidal gold as a probe. *Cell Mol. Neurobiol.* **5**, 271–284.

Deller T., Mundel P. and Frotscher M. (2000a) Potential role of synaptopodin in spine motility by coupling actin to the spine apparatus. *Hippocampus* **10**, 569–581.

Deller T., Merten T., Roth S. U., Mundel P. and Frotscher M. (2000b) Actin-associated protein synaptopodin in the rat hippocampal formation: localization in the spine neck and close association with the spine apparatus of principal neurons. *J. Comp. Neurol.* **418**, 164–181.

Deller T., Korte M., Chabanis S. *et al.* (2003) Synaptopodin-deficient mice lack a spine apparatus and show deficits in synaptic plasticity. *Proc. Natl Acad. Sci. USA* **100**, 10 494–10 499.

Dobrosotskaya I. and Guy R. K. and James G. L. (1997) MAGI-1, a membrane-associated guanylate kinase with a unique arrangement of protein–protein interaction domains. *J. Biol. Chem.* **272**, 31 589–31 597.

Engert F. and Bonhoeffer T. (1999) Dendritic spine changes associated with hippocampal long-term synaptic plasticity. *Nature* **399**, 19–21.

Fifkova E., Markham J. A. and Delay R. J. (1983) Calcium in the spine apparatus of dendritic spines in the dentate molecular layer. *Brain Res.* **266**, 163–168.

Fukazawa Y., Saitoh Y., Ozawa F., Ohta Y., Mizuno K. and Inokuchi K. (2003) Hippocampal LTP is accompanied by enhanced F-actin content within the dendritic spine that is essential for late LTP maintenance *in vivo*. *Neuron* **38**, 447–460.

Golding M. and Segal M. (2003) Protein kinase C and ERK involvement in dendritic spine plasticity in cultured rodent hippocampal neurons. *Eur. J. Neurosci.* **17**, 2529–2539.

Goode N. P., Shires M., Crellin D. M., Khan T. N. and Mooney A. F. (2004) Post-embedding double-labeling of antigen-retrieved ultrathin sections using a silver enhancement-controlled sequential immunogold (SECSI) technique. *J. Histochem. Cytochem.* **52**, 141–144.

Gray E. G. (1959) Axo-somatic and axo-dendritic synapses of the cerebral cortex: an electron microscopic study. *J. Anat.* **83**, 420–423.

Harris K. M., Fiala J. C. and Ostroff L. (2003) Structural changes at dendritic spine synapses during long-term potentiation. *Philos. Trans. R. Soc. Lond. B Biol. Sci.* **358**, 745–748.

Hering H. and Sheng M. (2001) Dendritic spines: structure, dynamics and regulation. *Nat. Rev. Neurosci.* **2**, 880–888.

Hirao K., Hata Y., Ide N., Takeuchi M., Irie M., Yao I., Deguchi M., Toyoda A., Sudhof T. C. and Takai Y. (1998) A novel multiple PDZ. domain-containing molecule interacting with *N*-methyl-D-aspartate receptors and neuronal cell adhesion proteins. *J. Biol. Chem.* **273**, 21 105–21 110.

Ichimura K., Kurihara H. and Sakai T. (2003) Actin filament organization of foot processes in rat podocytes. *J. Histochem. Cytochem.* **51**, 1589–1600.

Kaplan J. M., Kim S. H., North K. N. *et al.* (2000) Mutations in ACTN4, encoding α-actinin-4, cause familial focal segmental glomerulosclerosis. *Nat. Genet.* **24**, 251–256.

Kos C. H., Le T. C., Sinha S., Henderson J. M., Kim S. H., Sugimoto H., Kalluri R., Gerszten R. E. and Pollak M. R. (2003) Mice deficient in α-actinin-4 have severe glomerular disease. *J. Clin. Invest.* **111**, 1683–1690.

Kremerskothen J., Teber I., Wendholt D., Liedtke T., Bockers T. M. and Barnekow A. (2002) Brain-specific splicing of α-actinin 1 (ACTN1) mRNA. *Biochem. Biophys. Res. Commun.* **295**, 678–681.

Kremerskothen J., Plaas C., Buther K., Finger I., Veltel S., Matanis T., Liedtke T. and Barnekow A. (2003) Characterization of KIBRA, a novel WW domain-containing protein. *Biochem. Biophys. Res. Commun.* **300**, 862–867.

Laemmli U. K. (1970) Cleavage of structural proteins during the assembly of the head of bacteriophage T4. *Nature* **227**, 680–685.

Lamprecht R. and LeDoux J. (2004) Structural plasticity and memory. *Nat. Rev. Neurosci.* **5**, 45–54.

Matus A. (2000) Actin-based plasticity in dendritic spines. *Science* **290**, 754–758.

McCarthy J. B. and Millner T. A. (2003) Dendritic ribosomes suggest local protein synthesis during estrous synaptogenesis. *Neuroreport* **14**, 1357–1360.

Mundel P., Heid H. W., Mundel T. M., Kruger M., Reiser J. and Kriz W. (1997) Synaptopodin: an actin-associated protein in telencephalic dendrites and renal podocytes. *J. Cell Biol.* **139**, 193–204.

Patrie K. M., Drescher A. J., Welihinda A., Mundel P. and Margolis B. (2002) Interaction of two actin-binding proteins, SYNPO and α-actinin-4, with the tight junction protein MAGI-1. *J. Biol. Chem.* **277**, 30 183–30 190.

Sheng M. and Kim M. J. (2002) Postsynaptic signalling and plasticity mechanisms. *Science* **298**, 776–780.

Spacek J. (1985) Three-dimensional analysis of dendritic spines. II. Spine apparatus and other cytoplasmic components. *Anat. Embryol. (Berl.)* **171**, 235–243.

Spacek J. and Harris K. M. (1997) Three-dimensional organization of smooth endoplasmic reticulum in hippocampal CA1 dendrites and dendritic spines of the immature and mature rat. *J. Neurosci.* **17**, 190–203.

Toni N., Buchs P. A., Nikonenko I., Bron C. R. and Muller D. (1999) LTP promotes formation of multiple spine synapses between a single axon terminal and a dendrite. *Nature* **402**, 421–425.

Walikonis R. S., Jensen O. N., Mann M., Provance D. W. Jr, Mercer J. A. and Kennedy M. B. (2000) Identification of proteins in the postsynaptic density fraction by mass spectrometry. *J. Neurosci.* **20**, 4069–4080.

Weide T., Bayer M., Koster M., Siebrasse J. P., Peters R. and Barnekow A. (2001) The Golgi matrix protein GM130: a specific interacting partner of the small GTPase rab1b. *EMBO Report* **2**, 336–341.

Weins A., Schwarz K., Faul C., Barisoni L., Linke W. A. and Mundel P. (2001) Differentiation- and stress-dependent nuclear cytoplasmic redistribution of myopodin, a novel actin-bundling protein. *J. Cell Biol.* **155**, 393–404.

Wyszynski M., Kharazia V., Shanghvi R., Rao A., Beggs A. H., Craig A. M., Weinberg R. and Sheng M. (1998) Differential regional expression and ultrastructural localization of α-actinin-2, a putative NMDA receptor-anchoring protein, in rat brain. *J. Neurosci.* **118**, 1383–1392.

Yamazaki M., Matsuo R., Fukazawa Y., Ozawa F. and Inokuchi K. (2001) Regulated expression of an actin-associated protein, synaptopodin, during long-term potentiation. *J. Neurochem.* **79**, 192–199.

Yuste R. and Bonhoeffer T. (2001) Morphological changes in dendritic spines associated with long-term synaptic plasticity. *Annu. Rev. Neurosci.* **24**, 1071–1089.

